Journal of Solid State Chemistry 183 (2010) 327–331

Contents lists available at ScienceDirect

Journal of Solid State Chemistry

journal homepage: www.elsevier.com/locate/jssc

Non-stoichiometric Fe_xWN_2: Leaching of Fe from layer-structured $FeWN_2$

Akira Miura [a], Xiao-Dong Wen [a], Hideki Abe [b], Grace Yau [a], Francis J. DiSalvo [a,*]

[a] Department of Chemistry and Chemical Biology, Baker Laboratory, Cornell University, Ithaca, New York 14853-1301, USA
[b] National Institute for Materials Science (NIMS), 1-2-1 Sengen, Tsukuba, Ibaraki 305-0047 NIMS, Japan

ARTICLE INFO

Article history:
Received 8 September 2009
Received in revised form
9 November 2009
Accepted 10 November 2009
Available online 14 November 2009

Keywords:
Nitride
Deintercalation
Soft chemistry
Magnetic property
Electronic structure

ABSTRACT

Non-stoichiometric Fe_xWN_2 ($x \sim 0.72$) was synthesized via leaching of Fe from layer-structured stoichiometric $FeWN_2$ by soaking in sulfuric acid at ca. 50 °C. The synthesized products were characterized by powder X-ray diffraction (pXRD), secondary electron microscopy (SEM), energy dispersive X-ray analysis (EDX) and magnetic measurements. Non-stoichiometric Fe_xWN_2 has the same symmetry unit cell as stoichiometric $FeWN_2$ ($P6_3/mmc$), but the lattice parameters change: the *a*-axis expands by 0.16% while the *c*-axis decreases by 1.5%. Polycrystalline powder of Fe_xWN_2 showed similar morphologies as those of $FeWN_2$. The calculated electronic structure of stoichiometric $FeWN_2$ shows a more ionic-bonding character between Fe and N than that between W and N, which presumably allows for the partial Fe leaching from between the W–N prismatic layers. The magnetic susceptibility of Fe_xWN_2 smoothly decreases with increasing temperature from 3 to 300 K, unlike the broad maximum seen near 27 K in stoichiometric $FeWN_2$.

1. Introduction

Iron-based compounds and composites, including oxides, nitrides and arsenides, have been extensively studied due to the great natural abundance of iron and to the useful magnetic, catalytic and superconductive properties of such materials [1–10]. $FeWN_2$ is a layered nitride, consisting of alternating W–N prismatic layers and Fe (Fig. 1) [11–13]. The layer stacking is AcAc′BcBc′A, where capital letters represent a close packed nitrogen layer, lower case letters are close packed W layers and primed lower case letters Fe layers. It is easily synthesized by ammonolysis of $FeWO_4$ under flowing NH_3 at 700–800 °C. $FeWN_2$ powder shows metallic conductivity [12] and its susceptibility suggest antiferromagnetic or spin glass behavior [13]. It is reported to be stable in air and moisture, and does not dissolve in acids or bases [12]. The electronic structure of $FeWN_2$ has not been reported. $(Fe_{0.8}W_{0.2})WN_2$ is synthesized by ammonolysis of $Fe_2(WO_4)_3$ at 700 °C, where the Fe layer in $FeWN_2$ is now occupied by 20% W and 80% Fe [14]. $(Fe_{0.8}Mo_{0.2})MoN_2$ is also synthesized in a similar way [15].

Intercalation/deintercalation and exchange reactions involving alkali metals are typical low-temperature reactions expected in layered compounds. In the nitride system, intercalation and/or deintercalation of Li or Na into/from $LiWN_2$, $LiMoN_2$ and $NaTaN_2$ have also been reported [16,17]. The synthesis of $CuTaN_2$ is carried out by an exchange reaction using CuI at 400 °C with the formation of NaI as a by-product [18]. Intercalation of other transition metals including iron into hexagonal graphite-like BN is also reported [19]. However, to our knowledge, deintercalation of iron has not been reported from nitrides or from oxides. A few exchange reactions in layered oxides are known to replace alkali metals by $(Fe^{2+}Cl)^+$, but no reports of iron deintercalation have been published [20,21].

Our first interest in $FeWN_2$ was its possible utility as an electrocatalyst for oxygen reduction in proton exchange membrane fuel cells [8]. However, electrochemical testing did not reveal any significant catalytic activity. Rather, leaching of iron in the acidic electrolyte was observed. This iron removal is interesting since it would likely change the physical or chemical properties of that nitride. Since the intercalation/deintercalation should be reversible reactions and the reversibility of iron removal and insertion was not confirmed, here we term this phenomenon as leaching, not deintercalation. Here, we report the synthesis, morphology, crystal structure and magnetic properties of non-stoichiometric Fe_xWN_2 produced by leaching of Fe from stoichiometric $FeWN_2$. The electronic structure of stoichiometric $FeWN_2$ was calculated to help understand these observations.

2. Experimental details

$FeWO_4$ was first prepared by precipitation from an aqueous solution of $FeCl_2$ (Alfa Aesar, 99.5%) that was added into an aqueous solution of $Na_2WO_4 \cdot 2H_2O$ (Mallinckrodt). Black stoichiometric $FeWN_2$ powder was then synthesized by ammonolysis of the

* Corresponding author. Fax: +1 607 255 4137.
E-mail address: fjd3@cornell.edu (F.J. DiSalvo).

0022-4596/$ - see front matter © 2009 Elsevier Inc. All rights reserved.
doi:10.1016/j.jssc.2009.11.014

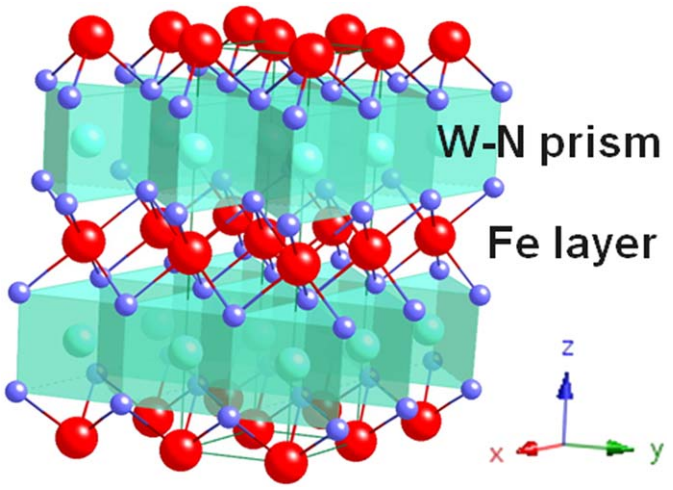

Fig. 1. Crystal structure for $FeWN_2$. Trigonal prismatic tungsten layers are shown as filled polyhedra. The iron and nitrogen positions are indicated in a ball and stick representation. Large and small balls represent iron and nitrogen, respectively.

precipitated $FeWO_4$ under flowing NH_3 gas at 700 °C for 12 h [11–13]. Non-stoichiometric Fe_xWN_2 was produced by soaking the synthesized $FeWN_2$ (100–300 mg) in 3 M sulfuric acid (ca. 20 ml) for 1–24 h at ca. 50 °C. After the acid treatment, the black powder was filtered, washed with water and isopropanol several times and dried at room temperature. The Fe_xWN_2 for magnetic measurements was dried at room temperature under vacuum for 24 h.

The reactivity of $FeWN_2$ toward 6M nitric acid and 6M hydrochloric acid was also examined in the same way. The reactivity of $FeWN_2$ toward I_2 and NO_2BF_4 was investigated by soaking $FeWN_2$ (ca. 100 mg) in acetonitrile (Mallinckrodt, 99.8%) with two-molar excess of I_2 (Fisher Scientific, 99.9%) or NO_2BF_4 (Acros Organic, 97%) at room temperature.

Powder X-ray diffraction (pXRD; Scintag XDS 2000; Cu $K\alpha$ radiation) was used for structural characterization. The scan range and step size were 10–120° and 0.02°, respectively. The d values of peak positions were determined by the peak search algorithm in Jade (Material data, Inc.), and we checked that the peak fitting was accurate for all intense peaks. Lattice parameters were calculated by the d values of the indexed peaks in the 2θ range of 30–120° of the samples mixed with Si powder, but not using two broad and highly asymmetric 118 and 212 diffraction peaks. Rietveld analysis was not performed since the layered habit of the crystallites leads to preferred orientation. Images of the samples on an Al support were taken with a scanning electron microscope (SEM; LEO-1550 field emission SEM) with energy dispersive X-ray analysis (EDX). Magnetic data was collected using a superconducting quantum interface device (SQUID; Quantum Design MPMS) at temperatures from 3 to 300 K in an applied filed of 5 kG.

The amount of Fe^{2+} ion in the remaining sulfuric acid solution was determined by optical absorbance of the 1,10-phenanthroline iron complex at 510 nm (Beckman DU640B Spectrophotometer) after neutralizing with 1.5 M NaOH and buffering to a pH of ca. 3.5 [22]. The total amount of Fe^{2+} and Fe^{3+} in the solution was measured in the same procedure as for Fe^{2+} ion, except that $NH_2OH \cdot HCl$ was not added as a reducing agent. The following chemicals were used: 1,10-phenanthroline (Aldrich 99+%), $NH_2OH \cdot HCl$ (Mallinckrodt 96.0%), anhydrous citric acid (Fisher Scientific 100%), dehydrate sodium citrate (Mallinckrodt 99.7%), NaOH (Mallinckrodt, 99%), and $Fe(NH_4)_2(SO_4)_2 \cdot 6H_2O$ (Mallinckrodt).

The computational calculations of electronic structure of $FeWN_2$ were based on density functional theory (DFT) method using the Vienna Ab-initio Simulation Package (VASP) [23–25]. The projected-augmented wave (PAW) [26,27] method with PBE pseudo-potential was employed. All calculations included spin polarization, also a $2 \times 2 \times 2$ supercell, a 500 eV energy cutoff for plane waves and a $(10 \times 10 \times 5)$ set of Monkhorst Pack grid of k-points. A supercell of $Fe_8W_8N_{16}$ was used in a calculation that allows for ferromagnetic (FM) or antiferromagnetic (AFM) ordering. The structural parameters (atomic position, lattice constants, and symmetry) were relaxed.

3. Results and discussion

After soaking $FeWN_2$ in sulfuric acid, no color change was observed in either $FeWN_2$ or in the solution. Fig. 2 shows pXRD patterns of $FeWN_2$ before (untreated $FeWN_2$) and after soaking in the acid for different times (acid-treated $FeWN_2$). pXRD patterns of both untreated and acid-treated $FeWN_2$ are indexed on a hexagonal structure unit cell. The inset shows that the 004 and 100 peaks are shifted toward higher and lower angles, respectively, as soaking time increased. The broader 004 peak after 1 h- and 3 h-acid-treated treatments suggests two phase behavior, while the sharper 004 peak after 24 h suggests that the sample is now almost single phase.

Table 1 shows the lattice parameters and Fe/W ratios semi-quantitatively determined by EDX. The lattice parameters of untreated $FeWN_2$ (a=2.8702(5) Å, c=10.989(5) Å) are close to the reported values (a=2.87630(5) Å, c=10.9320(4) Å [12]). The acid treatment increases the a-axis of $FeWN_2$ up to 0.16% with the soaking time, and decreases the c-axis of $FeWN_2$ by 1.5%. As a result, the volume of the unit cell decreased by 1.1%. The Fe/W ratio decreased from 1.02(4) to 0.75(4) after 1-hr acid treatment but further treatment evidenced no further significant change.

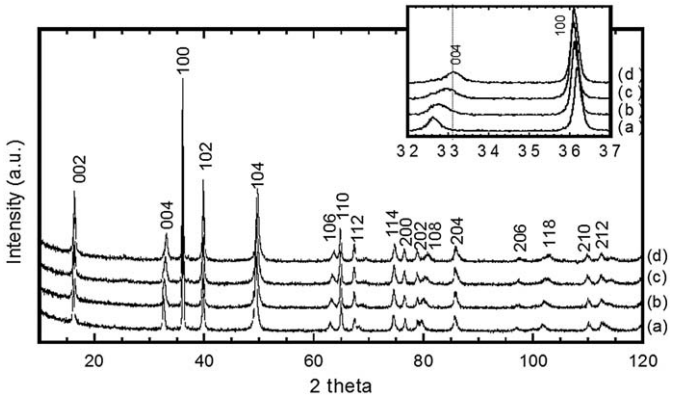

Fig. 2. pXRD patterns of $FeWN_2$ (a) before and after soaking in 3M sulfuric acid at 50 °C for (b) 1 h, (c) 3 h and (d) 24 h. Inset is a magnification of the 004 and 100 peaks.

Table 1
Lattice parameters and Fe/W ratio of untreated and 3 M sulfuric acid-treated $FeWN_2$ at 50 °C for different periods of time.

Time (h)	Lattice parameters (Å)		Volume (Å^3)	Fe/W
	a	c		
0 (untreated)	2.8702(5)	10.989(5)	78.41(5)	1.02(4)
1	2.8722(4)	10.950(4)	78.23(4)	0.75(4)
3	2.8739(6)	10.878(5)	77.81(5)	0.72(4)
24	2.8748(10)	10.829(9)	77.51(8)	0.72(6)

The amount of Fe^{2+} ion in sulfuric acid solution after the 24 h acid treatment was 29(1) % of the Fe in stoichiometric $FeWN_2$, which corresponds within error to the lower Fe/W ratio in the acid-treated product as determined by EDX. The absence of Fe^{3+} in the solution was confirmed by the measurement of the total amount of Fe^{2+} and Fe^{3+} ions, which was the same as the amount of Fe^{2+} ion within error. The EDX spectra showed an obvious nitrogen signal but a very weak to no oxygen signal both with or without acid treatment, suggesting that the materials are nitrides. We cannot preclude the possibility of small amount of oxygen incorporation or nitrogen deficiency because EDX is not very sensitive to oxygen and nitrogen quantities.

The morphologies of both the untreated and acid-treated $FeWN_2$ were similar: aggregated plate crystals of 0.5–1 μm in length and ca. 50 nm in thickness (Fig. 3). Some of the crystals showed hexagonal shape, indicating the layers are parallel to the hexagonal surface of the plate crystals.

Since $FeWN_2$ consists of alternating layers of W and Fe, the acid treatment is believed to partially remove Fe from the Fe layer, resulting in non-stoichiometric Fe_xWN_2 with Fe vacancies. Charge balance could be maintained by oxidation of iron/tungsten, formation of a hole in the valence band, and/or incorporation of protons.

The lattice parameters and the shape of pXRD peaks gradually changed with the soaking time in sulfuric acid from 1 to 24 h, but the Fe/W ratio as determined by EDX decreased in 1 h and did not decrease significantly on further soaking. This result indicates that the diffusion of Fe is relatively slowly. First, inhomogeneous Fe_xWN_2 is formed, which is suggested by the broadened pXRD 004 peak for 1 and 3 h-acid-treated samples. Since the Fe layer is parallel to the face of the plate crystals, leaching occurs from the edge of the plate crystals, resulting in inhomogeneous Fe_xWN_2. The sample became homogeneous through solid-state diffusion after 24 h. Minor changes in lattice parameters and peak shape are a common feature in other intercalated/deintercalated compounds [16,17].

The reaction of $FeWN_2$ with various acids and oxidants was also examined (Table 2). We can categorize them into three groups, based on pXRD and EDX results. The first one is iodine, which did not result in significant changes in terms of lattice parameters and composition. The second group includes hydrochloric acid. Hydrochloric acid treatment slightly changed the lattice parameters and decreased the Fe/W ratio, by an amount similar to that of the sulfuric acid treatment. When $FeWN_2$ was soaked in 6 M hydrochloric acid, the solution clearly turned yellow, perhaps due to the formation and dissolution of $FeCl_3$. Thus, the leaching of Fe is believed to occur by this hydrochloric acid treatment. The Fe/W ratio after hydrochloric acid treatment after 72 h was the same as that after sulfuric acid treatment within error, implying that the end point of leaching in the non-stoichiometric nitride, Fe_xWN_2, is obtained when x is close to 0.7. The third group contains nitric acid and NO_2BF_4, both of which form oxides and decomposed the framework of $FeWN_2$. Acid-treatment in 6 M nitric acid solution resulted in the immediate formation of bubbles. After 24 h, a yellow precipitate was left, which was identified as $WO_3 \cdot H_2O$ by pXRD. When $FeWN_2$ was soaked in acetonitrile with a 2-molar excess NO_2BF_4 solution, bubbles were also observed and a black powder was obtained after 48 h. pXRD of the NO_2BF_4-treated $FeWN_2$ showed shifted peaks of $FeWN_2$ (similar to sulfuric acid-treated $FeWN_2$) and an amorphous broad peak around 28°. Low Fe/W (0.22(2)) and apparent oxygen signal were found by EDX, indicating that the product is a mixture of amorphous tungsten oxide/hydroxide and non-stoichiometric Fe_xWN_2.

The electronic structures of ferromagnetic (FM) and antiferromagnetic (AFM) $FeWN_2$ were calculated. The magnetic interaction of Fe in AFM FeWN is assumed to be largest within the layer. The optimized lattice parameters of FM and AFM $FeWN_2$ (FM: a=2.895 Å, c=10.969 Å, AFM: a=2.890 Å, c=11.025 Å) were close to experimental ones (a=2.8702(5) Å, c=10.989(5) Å). When half of the Fe was removed from the FM $FeWN_2$, the optimized a-axis increased by 0.5% while the c-axis decreased by 7%. The increase of the a-axis and the decrease of c-axis follows the same trends as the experimental ones, though the assumed level of

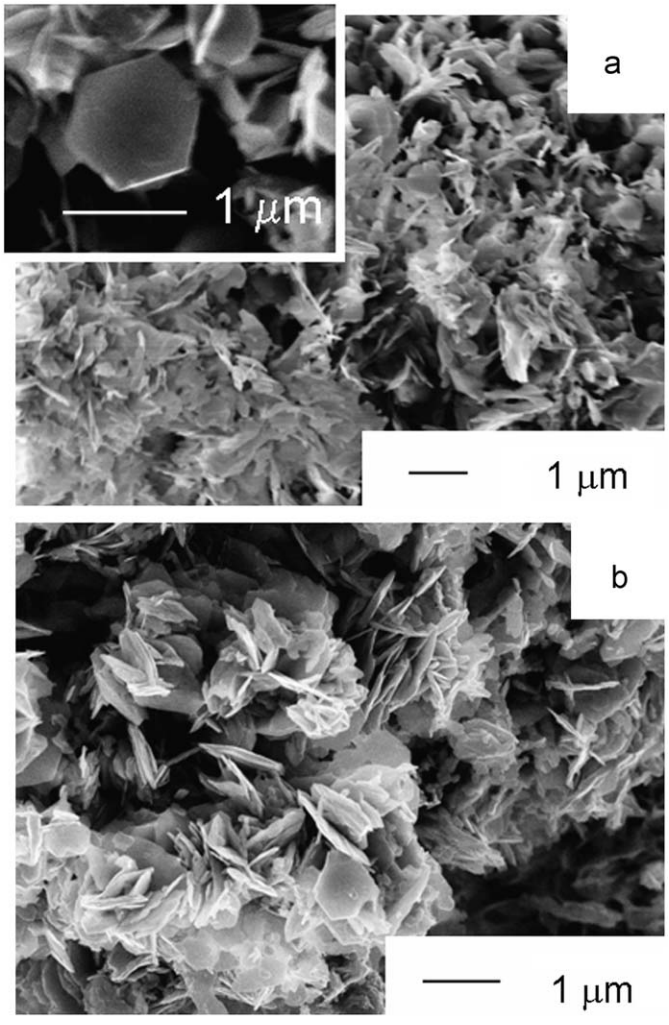

Fig. 3. SEM pictures of $FeWN_2$ (a) before and (b) after soaking in 3M sulfuric acid at 50 °C for 24 h. Inset is a thin crystal plate showing the hexagonal plane.

Table 2
Summary of lattice parameters and Fe/W ratio from the reaction of $FeWN_2$ with various acids and oxidizing agents.

Compound	Temp. (°C)	Time (h)	Lattice parameters (Å)		Volume (Å^3)	Fe/W
			a	c		
Untreated	–	–	2.8702(5)	10.989(5)	78.41(5)	1.02(4)
I_2/AN	RT.	48	2.8716(4)	10.968(8)	78.33(4)	0.92(4)
6M HCl	50	24	2.8760(10)	10.840(8)	77.65(7)	0.84(3)
6M HCl	50	72	2.875(1)	10.811(6)	77.42(7)	0.71(5)
NO_2BF_4/AN	RT.	48	2.8710(7)[a]	10.869(12)[a]	77.64(10)[a]	0.22(2)
6M HNO_3	50	24	WO_3 (H_2O)	–	–	

AN: acetonitrile, R.T: room temperature.

[a] Existence of amorphous phase (a broad pXRD peak around 28°).

removed Fe is approximately twice that observed, and the calculated decrease of the *c*-axis is much higher than observed.

The energy of AFM $FeWN_2$ is slightly higher than FM one (0.06 eV/$FeWN_2$ unit). This is inconsistent with the observed antiferromagnetic behavior [13], which can be attributed to the assumed antiferromagnetic structure or to inherent small errors in DFT calculations [28]. Here, an electronic structure of AFM $FeWN_2$ is shown (Fig. 4). The total density of states (TDOS) of AFM $FeWN_2$ indicates that the nitride is metallic, which agrees with experimental results [12]. The contributions to the TDOS were explored by utilizing partial density of states (PDOS). For both Fe and W, the *d*-orbitals (up and down spins) cross the Fermi level. Nonetheless, there are asymmetric up and down states on the Fe atoms, while there are symmetric states in the W atoms. This indicates that the magnetic moments are attributed to the Fe atoms, as expected. It is noted that the Fe *d* orbitals are more localized, while the W *d* orbitals are more delocalized. In addition, the N main 2*p* orbitals fall between -8 and -4 eV below the Fermi level; the main peak of Fe *d* orbital character ($-4 \sim 4$ eV) is above the N 2*p* valence bands. The result indicates that Fe–N and W–N bonds have more ionic and covalent bonding characters, respectively. This bonding feature is similar to that of Li–N and Mo–N bonds in the layered nitride $LiMoN_2$ [29], from which the Li ion can be removed by using oxidants [16]. This is likely related to the ability of Fe to leach into acid solution. These ionic and covalent bonding characters for Fe–N and W–N, respectively, were also observed in the DOS of FM $FeWN_2$.

The susceptibility of non-stoichiometric Fe_xWN_2 smoothly decreased with increasing temperature from 3 to 300 K (Fig. 5), but does not obey the modified Curie–Weiss equation ($\chi_{Fe\ mol}=\chi_0+C/(T-\theta)$, where χ_{mol} is susceptibility per Fe mol, χ_0 is constant, C is Curie temperature, T is temperature (K), and θ is Weiss temperature (K)). Consequently, it is not possible to easily extract a magnetic moment per Fe from this data. The susceptibility behavior is different from that of $FeWN_2$, which shows a maximum at 27 K. The magnitude of the susceptibility per mole of Fe for non-stoichiometric Fe_xWN_2 (x=0.72) is almost the same as that of $FeWN_2$.

A simple two point conductivity measurement was performed before and after 24 h-sulfuric acid treatment by pressing powders (9.34 mm diameter and 1.22 mm thickness) between two metal rods in an insulating tube at room temperature under air. The

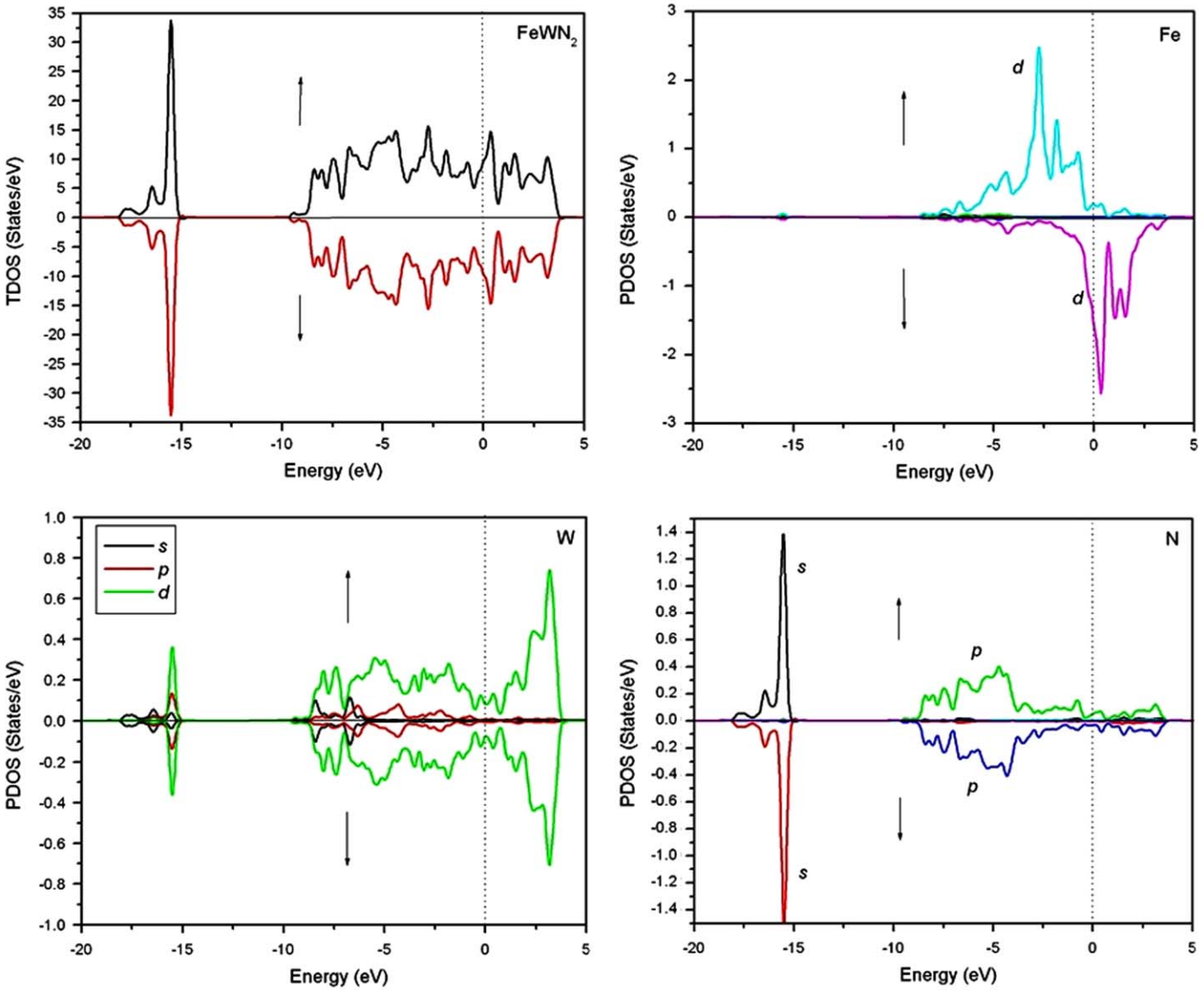

Fig. 4. Calculated density of states (DOS) of the antiferromagnetic $FeWN_2$ supercell (8 $FeWN_2$) structure. The projected partial density of states (PDOS) of one Fe, W and N atom are shown. The dotted line indicates the adjusted Fermi level at 0 eV. Note that the DOS scales are different.

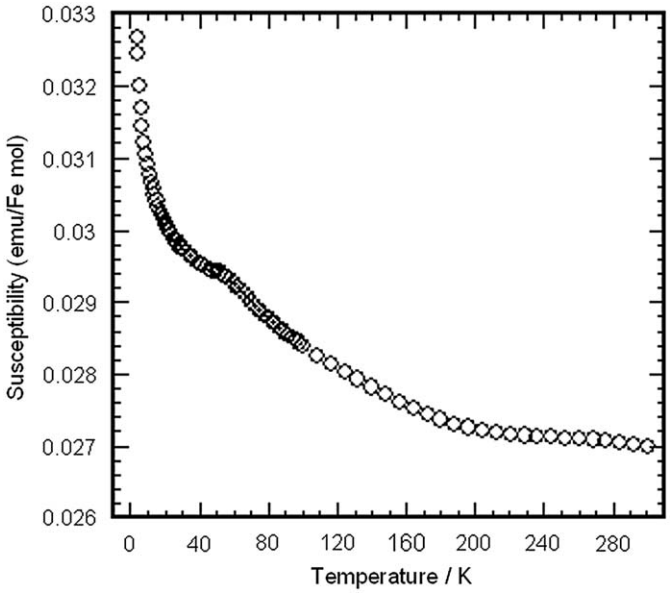

Fig. 5. Temperature dependence of magnetic susceptibility of $FeWN_2$ after 24 h sulfuric acid treatment.

conductivities of pressed powder samples were essentially the same before and after the sulfuric acid treatment: 0.3 S/cm. This conductivity is the same order of that in the previous report of $FeWN_2$ (ca.0.6 S/cm) [12], which is measured by four point measurement of a pressed powder sample. The major limitation of these measurements is that the conductivity can be dominated by the contact resistance between particles. Consequently, we can give only a lower limit of conductivity, which may be dominated not by the intrinsic conductivity of bulk Fe_xWN_2.

In conclusion, Fe leaching via soaking stoichiometric $FeWN_2$ in sulfuric and hydrochloric acids produced non-stoichiometric Fe_xWN_2. The partial removal of iron caused by sulfuric acid treatment produced minor structural and negligible morphological changes. We hypothesize that this leaching occurs from the Fe layer rather than the W layer, since the Fe–N bonding is more ionic than the W–N bonding.

Supplementary material

Typical EDX spectra for $FeWN_2$ and Fe_xWN_2(x=0.72), pXRD patterns of $FeWN_2$ reacted with I_2, HCl, HNO_3 and NO_2BF_4, structure models for computational calculations, and DOS and pDOS of FM $FeWN_2$ are presented in supplementary material.

Acknowledgments

A.M. acknowledges Hongsen Wang for testing the activity of $FeWN_2$/C composite as a possible fuel cell catalyst and Yongkwan Dong for fruitful discussions. A.M. acknowledges Malcolm Thomas at the Cornell Center for Materials Research for help with the SEM data collection. This work was supported by NSF through grant number DMR-0602526.

Appendix A. Supplementary material

Supplementary data associated with this article can be found in the online version at doi:10.1016/j.jssc.2009.11.014.

References

[1] Y. Zheng, Y. Cheng, Y. Wang, F. Bao, L. Zhou, X. Wei, Y. Zhang, Q. Zheng, J. Phys. Chem. B 110 (2006) 3093–3097.
[2] I. Cesar, A. Kay, J.A. Gonzalez Martinez, M. Gratzel, J. Am. Chem. Soc. 128 (2006) 4582–4583.
[3] Y. Tsujimoto, C. Tassel, N. Hayashi, T. Watanabe, H. Kageyama, K. Yoshimura, M. Takano, M. Ceretti, C. Ritter, W. Paulus, Nature 450 (2007) 1062–1065.
[4] B. Eck, R. Dronskowski, M. Takahashi, S. Kikkawa, J. Mater. Chem. 9 (1999) 1527–1537.
[5] K.H. Jack, Proceedings of the Royal Society of London Series a—Mathematical and Physical Sciences 195 (1948) 34–40.
[6] A. Houben, V. Šepelak, K.-D. Becker, R. Dronskowski, Chem. Mater. 21 (2009) 784–788.
[7] C.J.H. Jacobsen, Chem. Commun. (2000) 1057–1058.
[8] M. Lefevre, E. Proietti, F. Jaouen, J.P. Dodelet, Science 324 (2009) 71–74.
[9] Y. Kamihara, H. Hiramatsu, M. Hirano, R. Kawamura, H. Yanagi, T. Kamiya, H. Hosono, J. Am. Chem. Soc. 128 (2006) 10012–10013.
[10] Y. Kamihara, T. Watanabe, M. Hirano, H. Hosono, J. Am. Chem. Soc. 130 (2008) 3296–3297.
[11] D.S. Bem, H-C zur Loye, J. Solid State Chem. 104 (1993) 467–469.
[12] D.S. Bem, C.M. Lampe-Önnerud, H.P. Olsen, H-C zur Loye, Inorg. Chem. 35 (1996) 581–585.
[13] D.S. Bem, J.D. Houmes, H-C zur Loye, In: A.R. Barron, G.S. Fischman, M.A. Fury, A.F. Hepp (Eds.), MRS Symposium Proceeding, Covalent Ceramics II: Non-Oxides, Boston, 1993, vol. 327, pp. 153–162.
[14] J.D. Houmes, S. Deo, H-C zur Loye, J. Solid State Chem. 131 (1997) 374–378.
[15] D.S. Bem, H.P. Olsen, H-C zur Loye, Chem. Mater. 7 (1995) 1824–1828.
[16] S.H. Elder, L.H. Doerrer, F.J. DiSalvo, J.B. Parise, D. Guyomard, J.M. Tarascon, Chem. Mater. 4 (1992) 928–937.
[17] P.E. Rauch, F.J. DiSalvo, J. Solid State Chem. 100 (1992) 160–165.
[18] U. Zachwieja, H. Jacobs, Eur. J. Solid State Inorg. Chem. 28 (1991) 1055–1062.
[19] E. Budak, C. Bozkurt, J. Solid State Chem. 177 (2004) 1768–1770.
[20] H. Kageyama, L. Viciu, G. Caruntu, Y. Ueda, J.B. Wiley, J. Phys. Condens. Matter. 16 (2004) S585–S590.
[21] L. Viciu, G. Caruntu, N. Royant, J. Koenig, W.L. Zhou, T.A. Kodenkandath, J.B. Wiley, Inorg. Chem. 41 (2002) 3385–3388.
[22] Z. Marczenko, Spectrophotometric Determination of Element, Wiley, 1976, pp. 309–312.
[23] J.P. Perdew, K. Burke, M. Ernzerhof, Phys. Rev. Lett. 77 (1996) 3865–3868.
[24] J.P. Perdew, K. Burke, M. Ernzerhof, Phys. Rev. Lett. 78 (1997) 1396.
[25] G. Kresse, J. Hafner, Phys. Rev. B 47 (1993) 558–561.
[26] P.E. Blöchl, Phys. Rev. B 50 (1994) 17953–17979.
[27] G. Kresse, D. Joubert, Phys. Rev. B 59 (1999) 1758–1775.
[28] R. Hoffmann, P. von Ragué Schleyer, H.F. Schaefer III, Angew. Chem. Int. Ed. 47 (2008) 7164–7167.
[29] D.J. Singh, Phys. Rev. B 46 (1992) 9332–9335.